Cooperative Formation Flying Control Laws for Automatic Air to Air Refuelling

Rodney Rodríguez Robles⋆, Diego Lodares Gómez⋆ and Francisco Asensio Nieto⋆
⋆*Airbus Defence and Space*
Avda. de John Lennon, s/n, 28906 Getafe, Spain
rodney.rodriguez@airbus.com · diego.lodares@airbus.com · francisco.asensio@airbus.com

Abstract

This paper describes a Cooperative Control Law (CCL) with robust adaptive command and control algorithms for close formation flying of highly heterogeneous manned or unmanned assets (receivers) within the scope of Automatic Air to Air Refuelling (A3R) operations. The three main layers of the proposed CCL providing adaptive guidance, consensus and collision avoidance functionalities are described and formal stability demonstrations using Lyapunov theory are presented. Maturity and performance of the proposed algorithms is assessed via simulations of A3R operations. Results and conclusions are presented as well as some indications for future developments.

1. Introduction

A3R is a complex operation involving a set of heterogeneous manned and unmanned aircraft flying in close formation before, during and after the fuel transfer. Throughout these phases, trajectory commands emitted by either the Air Refuelling Operator (ARO) of the tanker aircraft, the pilot of a manned receiver, or the Air Vehicle Operator (AVO) of an unmanned receiver are substituted by computer-controlled trajectories. Autonomy levels of the A3R operation are defined by the responsibilities and tasks delegated to the computer, and range from Semi-Automatic Air to Air Refuelling to fully Autonomous Air to Air Refuelling, where the whole operation is performed without required human intervention.

In the last fifteen years there have been major breakthroughs in the field of one-to-one A3R, with flight test demonstrations of image recognition and control technologies implemented in the receiver aircraft [1, 2] and in the tanker aircraft [3, 4]. The next step towards a more autonomous operation including multiple manned and unmanned assets would require additional robust control and cooperative capabilities provided by the CCL to enable close formation flying with the required safety levels. Thus, in line with the A3R Concept of Operations (CONOPS) defined by the Aerial Refuelling Systems Advisory Group (ARSAG), autonomous close formation flying has been identified as one of the main enabling technologies in need of further development in order to reach the fully autonomous level of A3R [5].

In the autonomous A3R operation envisioned by Airbus Defence and Space, the proposed CCL for close formation flying is based on a tanker-centralized command and control architecture that maximizes the compatibility with any friendly receiver aircraft from a blue force, either manned or unmanned. In contrast with a decentralized control architecture, the proposed one requires no modifications of the receiver aircraft flight control software, under the hypothesis that the latter accept autopilot commands from exogenous sources via a low-latency, encrypted and secure military communication network. Following this approach, the tanker would act as a mothership generating the command and control signals to the autopilots of the receiver aircraft, while being responsible for granting the required safety standards during the whole A3R operation and providing an optimal refuelling scheduling of the assets, collision avoidance functionalities, and predefined separation protocols against loss of communication events.

The proposed CCL has been structured in a modular and hierarchical fashion, with three low-level command modules and a top-level management module. The first low-level module contains the 4D adaptive guidance algorithms that warrant a homogeneous response of the receiver aircraft position tracking error. The second module comprises the adaptive second-order consensus protocol in charge of switching communication topologies and attaining the desired coordination between the receivers. The third module contains the collision avoidance algorithm that ensures a minimum separation distance between all of the aircraft in the formation. Finally, these three modules are linked to a

top-level manager, which combines their outputs in order to generate command inputs to the autopilots of each one of the receiver aircraft part of the A3R operation.

With the aim of maximizing the compatibility of the CCL with the wide spectrum of receiver aircraft autopilot dynamics, this work focuses on the design of robust adaptive algorithms. By employing adaptive control and estimation strategies, the knowledge requirements of potentially classified information related to the performance and dynamic response of the receiver aircraft autopilots can be relaxed. Moreover, the adaptive approach has the inherent advantage of minimizing the design and upload of ad-hoc embedded flight control software for new receiver aircraft that were not considered during the design loops of non-adaptive control architectures. Nevertheless, versatility of the adaptive control and consensus algorithms occasionally comes at the expense of lower robustness and stability margins against unmodeled nonlinear dynamics and delays, which might not have been considered during the initial design phase of the CCL. Hence, it is mandatory to add robust control modifications to the adaptive algorithms and include learning protections against parameter drifting and bursting phenomena [6, 7].

2. A3R Concept of Operation

The A3R operational procedure will make use of the existing Air to Air Refuelling procedures and positions as extensively as possible to ensure interoperability during mixed manned/unmanned refuelling operations. Therefore, A3R receiver positions around the tanker are the same ones defined for manned operations [5] (*Echelon Left, Astern Left / Center / Right, Contact* and *Echelon Right*), with the inclusion of a new control point required to check navigation performance and communications status before clearing the receiver aircraft to *Echelon Left*. This new point is termed the *Transition Position*, located 1500ft behind and 1000ft below the tanker. The receiver approaches the *Transition Position* from the rendezvous re-joint position. All of these positions are depicted in Figure 1.
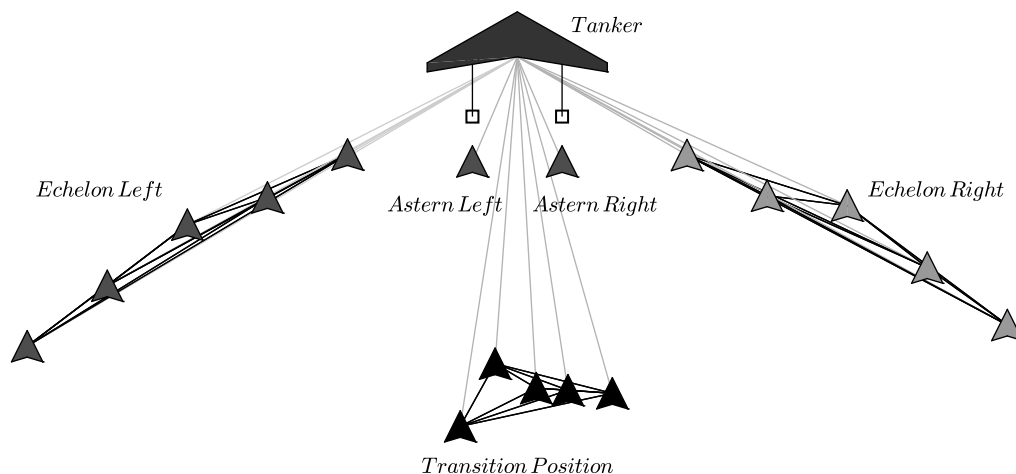

Figure 1: A3R operation positions. Grey lines indicate an undirected communication link between each receiver aircraft and the tanker via a data-link. Black lines denote a "virtual" undirected communication link solely generated by the tanker to coordinate each formation (consensus protocols).

In the proposed CCL architecture, only those formations of receiver aircraft at the *Transition Position*, *Echelon Left* and *Echelon Right* are coordinated via the guidance, consensus and collision avoidance modules. Receiver aircraft at *Astern Left, Center, Right* or in *Contact* receive commands only from the guidance and collision avoidance modules. This segregation intends to minimize the propagation of perturbations to receiver aircraft that are engaged in critical phases of the operation, where their main objective is not to fly in close formation, but to establish contact with a refuelling drogue or to accurately maintain a stationary relative position with the tanker in order to be refuelled by a boom system.

3. Adaptive Guidance

3.1 Dynamic Inversion

The guidance law for formation flight has the basic goal of making each of the aircraft follow a particular reference point defined by a position r_{ref}, velocity v_{ref}, acceleration a_{ref} and jerk $j_{ref} \triangleq da_{ref}/dt$. The proposed guidance law is based on performing a dynamic inversion on each plant, being all of them modelled as second order LPV (Linear Parameter Varying) systems

$$\dot{x} = Ax + Bu,$$
$$y = x, \tag{1}$$

where $A \in \mathbb{R}^{6 \times 6}$, $B \in \mathbb{R}^{6 \times 3}$, the pair $[A, B]$ is controllable; $x = [v, \chi, \gamma, \dot{v}, \dot{\chi}, \dot{\gamma}]^T \in \mathbb{R}^6$ is the state vector, $u = [v_{cmd}, \chi_{cmd}, \gamma_{cmd}]^T \in \mathbb{R}^3$ is the autopilot control input, $y \in \mathbb{R}^6$ is the measurement vector, v is the speed, χ the heading angle and γ the climb or flight-path angle. Aircraft kinematics can be expressed in the velocity-axes frame, with unit vectors $u_v, u_\chi, u_\gamma \in \mathbb{R}^3$,

$$u_v = \cos\chi \cos\gamma \, e_x + \sin\chi \cos\gamma \, e_y - \sin\gamma \, e_z,$$
$$u_\chi = -\sin\chi \, e_x + \cos\chi \, e_y, \tag{2}$$
$$u_\gamma = u_v \times u_\chi,$$

where $e_x, e_y, e_z \in \mathbb{R}^3$ are the unit vectors defining the local horizon (NED) frame. The vehicle's velocity v, acceleration a, and jerk $j \triangleq da/dt$ are given by

$$v = v \, u_v,$$
$$a = \dot{v} \, u_v + v\dot{\chi} \cos\gamma \, u_\chi - v\dot{\gamma} \, u_\gamma, \tag{3}$$
$$j = \left(\ddot{v} - v\dot{\gamma}^2 - v\dot{\chi}^2 \cos^2\gamma\right) u_v + \left(v\ddot{\chi}\cos\gamma + 2\dot{v}\dot{\chi}\cos\gamma - 2v\dot{\chi}\dot{\gamma}\sin\gamma\right) u_\chi - \left(v\ddot{\gamma} + 2\dot{v}\dot{\gamma} + v\dot{\chi}^2 \cos\gamma \sin\gamma\right) u_\gamma,$$

so that j can be expressed in terms of the time derivative of the state vector $\dot{x}$

$$j = \Phi\dot{x} + f(x),$$
$$\Phi = \left[\begin{array}{c|ccc} & 1 & 0 & 0 \\ 0_{3\times3} & 0 & v\cos\gamma & 0 \\ & 0 & 0 & -v \end{array} \right] = \left[\begin{array}{c|c} 0_{3\times3} & \phi \end{array} \right], \tag{4}$$
$$f(x) = \left[-v\dot{\gamma}^2 - v\dot{\chi}^2 \cos^2\gamma, \;\; 2\dot{v}\dot{\chi}\cos\gamma - 2v\dot{\chi}\dot{\gamma}\sin\gamma, \;\; -2\dot{v}\dot{\gamma} - v\dot{\chi}^2 \cos\gamma \sin\gamma \right]^T.$$

An expected guidance error (or *miss distance vector* [8]), $d \in \mathbb{R}^3$, can be defined as

$$d = (r_{ref} - r) + t_{go}(v_{ref} - v),$$
$$\dot{d} = (v_{ref} - v) + t_{go}(a_{ref} - a), \tag{5}$$
$$\ddot{d} = (a_{ref} - a) + t_{go}(j_{ref} - j).$$

The approach consists in establishing a desired second-order dynamics for d, homogeneous in all coordinates:

$$\ddot{d} + 2\xi_g\omega_g\dot{d} + \omega_g^2 d = 0, \;\; \text{ideally}, \tag{6}$$

where $\xi_g, \omega_g \in \mathbb{R}^+$ are some design damping and natural frequency. Using equations (1), (4), (5), (6), and carrying out the appropriate coordinate rotations, one can solve for the exact plant input that would achieve the desired guidance error dynamics (6):

$$u = (\Phi B)^{-1}\left(-\Phi Ax + F(x, r_{ref}, v_{ref}, a_{ref}, j_{ref})\right),$$
$$F(x, r_{ref}, v_{ref}, a_{ref}, j_{ref}) = -f(x) - \frac{a}{t_{go}} + \frac{1}{t_{go}} \left[\begin{array}{c} u_v^T \\ u_\chi^T \\ u_\gamma^T \end{array} \right] \left(j_{ref}t_{go} + a_{ref} + t_I v_{ref} + 2\xi_g\omega_g\dot{d} + \omega_g^2 d\right). \tag{7}$$

It is clear from (7) that a necessary condition for this control law to be realizable is that the product $(\Phi B) \in \mathbb{R}^{3\times3}$ should always be invertible.

3.2 Adaptive Control Laws

Indeterminations and changes in the A and B matrices of (1) affect the performance of the pure dynamic inversion law (7). In reality, what are known are the estimates of these matrices, $\hat{A}$ and $\hat{B}$ (the latter verifying to be invertible when premultiplied by Φ, as happened with B), with the support of a series-parallel modelization of the true plant

$$
\begin{aligned}
\dot{\hat{x}} &= A_m\hat{x} + (\hat{A} - A_m)x + \hat{B}u, \\
&= A_m\tilde{x} + \hat{A}x + \hat{B}u,
\end{aligned}
\tag{8}
$$

where A_m is a Hurwitz design matrix with the same dimensions as $\hat{A}$. Let the estimation errors be defined as $\tilde{x} = \hat{x} - x$, $\tilde{A} = \hat{A} - A$, and $\tilde{B} = \hat{B} - B$. Then, the state estimation error $\tilde{x}$ will conform to the following dynamics:

$$
\dot{\tilde{x}} = A_m\tilde{x} + \tilde{A}x + \tilde{B}u,
\tag{9}
$$

and the true input to the plant will be

$$
u = (\Phi\hat{B})^{-1}\left(-\Phi\hat{A}x + F(x, \text{r}_{\text{ref}}, \text{v}_{\text{ref}}, \text{a}_{\text{ref}}, \text{j}_{\text{ref}})\right),
\tag{10}
$$

where F and Φ are the same as in (7), given that all the variables involved in them (as well as the true and estimated state vectors x, $\hat{x}$) are assumed to be measurable. Since this true input will no longer cancel out all the terms necessary to achieve (6), one can define the departure from the desired error dynamics as

$$
\varepsilon \triangleq \ddot{d} + 2\xi_g\omega_g\dot{d} + \omega_g d = t_{go}\Phi\left(\tilde{A}x + \tilde{B}u\right),
\tag{11}
$$

and the definition of $D = \left[d^T,\ \dot{d}^T\right]^T$ leads to a state-space equation for the miss distance vector

$$
\dot{D} = A_g D + B_g\varepsilon,
$$
$$
A_g = \left[\begin{array}{c|c} 0_{3\times3} & I_{3\times3} \\ \hline -\omega_g^2 I_{3\times3} & -2\xi_g\omega_g I_{3\times3} \end{array}\right], \quad B_g = \left[\begin{array}{c} 0_{3\times3} \\ I_{3\times3} \end{array}\right],
\tag{12}
$$

where I is the identity matrix. The goal will be to derive an adaptive scheme that attempts to keep this quantity at bay, with satisfactory performance, by updating the estimated matrices $\hat{A}$ and $\hat{B}$ employed by control law (10).

3.2.1 Lyapunov-Based Design Law

The aforementioned objective can be met by defining Lyapunov function candidate

$$
V = \frac{1}{2}D^T P_D D + \frac{1}{2}\tilde{x}^T P_m\tilde{x} + \frac{1}{2}\text{tr}\left(\tilde{A}^T\Gamma_A^{-1}\tilde{A}\right) + \frac{1}{2}\text{tr}\left(\tilde{B}^T\Gamma_B^{-1}\tilde{B}\right),
\tag{13}
$$

where P_D, P_m, Γ_A, $\Gamma_B \in \mathbb{R}^{6\times6}$ are positive definite matrices, and tr is the trace operator. The time derivative of V, calculated using (12) and (9), is given by

$$
\begin{aligned}
\dot{V} =& \frac{1}{2}D^T\left(A_g^T P_D + P_D A_g\right)D + \frac{1}{2}\tilde{x}^T\left(A_m^T P_m + P_m A_m\right)\tilde{x} + \frac{1}{2}\left(\varepsilon^T B_g^T P_D D + D^T P_d B_g\varepsilon\right) \\
&+ \frac{1}{2}\left(\left(\tilde{A}x + \tilde{B}u\right)^T P_m\tilde{x} + \tilde{x}^T P_m\left(\tilde{A}x + \tilde{B}u\right)\right) + \text{tr}\left(\tilde{A}^T\Gamma_A^{-1}\dot{\hat{A}}\right) + \text{tr}\left(\tilde{B}^T\Gamma_B^{-1}\dot{\hat{B}}\right),
\end{aligned}
\tag{14}
$$

so that P_D and P_m should satisfy the following Lyapunov equations in order to verify the stability condition $\dot{V} \leq 0$:

$$
\begin{aligned}
A_g^T P_D + P_D A_g &= -Q_D, \\
A_m^T P_m + P_m A_m &= -Q_m,
\end{aligned}
\tag{15}
$$

with Q_D, $Q_m \in \mathbb{R}^{6\times6}$ being positive definite design matrices. Using (11) and (15), $\dot{V}$ can be written as

$$
\begin{aligned}
\dot{V} =& -\frac{1}{2}D^T Q_D D - \frac{1}{2}\tilde{x}^T Q_m\tilde{x} \\
&+ \text{tr}\left(\tilde{A}^T\left(\Gamma_A^{-1}\dot{\hat{A}} + \left(t_{go}\Phi^T B_g^T P_D D + P_m\tilde{x}\right)x^T\right)\right) \\
&+ \text{tr}\left(\tilde{B}^T\left(\Gamma_A^{-1}\dot{\hat{B}} + \left(t_{go}\Phi^T B_g^T P_D D + P_m\tilde{x}\right)u^T\right)\right),
\end{aligned}
\tag{16}
$$

indicating that the estimated parameter update laws that would yield a stable system should have the following form:

$$\dot{\hat{A}} = -\Gamma_A \left(t_{go}\Phi^T B_g^T P_D D + P_m \tilde{x}\right) x^T,$$
$$\dot{\hat{B}} = -\Gamma_B \left(t_{go}\Phi^T B_g^T P_D D + P_m \tilde{x}\right) u^T. \tag{17}$$

3.2.2 Bi-Objective Optimal Modification

Update laws (17) can be upgraded using optimal control theory [9], by making them include additional robustness terms. The modification comes from minimizing the infinite-time horizon cost function

$$J = \lim_{T\to\infty} \frac{1}{2} \int_0^T (D - \Delta_D)^T Q_D (D - \Delta_D) + (\tilde{x} - \Delta_m)^T Q_m (\tilde{x} - \Delta_m) \, \mathrm{d}t, \tag{18}$$

with Hamiltonian

$$H = \frac{1}{2}(D - \Delta_1)^T Q_D (D - \Delta_D) + \frac{1}{2}(\tilde{x} - \Delta_m)^T Q_m (\tilde{x} - \Delta_m) + \lambda^T \dot{D} + \mu^T \dot{\tilde{x}}, \tag{19}$$

where $\lambda(t) : [0, \infty) \to \mathbb{R}^6$ and $\mu(t) : [0, \infty) \to \mathbb{R}^6$ are the adjoint vectors of D and $\tilde{x}$ respectively, and $Q_m, Q_D \in \mathbb{R}^{6\times6}$ are positive definite matrices. The necessary conditions of optimality from Pontryagin's minimum principle provide the adjoint equations

$$\dot{\lambda} = -\left(\nabla_D H\right)^T = -Q_D(D - \Delta_D) - A_g^T \lambda, \ \dot{\mu} = -\left(\nabla_{\tilde{x}} H\right)^T = -Q_m(\tilde{x} - \Delta_m) - A_m^T \mu, \tag{20}$$

and the optimal control update laws can be obtained from the gradient-based formulas

$$\dot{\hat{A}}^T = -\left(\nabla_{\tilde{A}} H\right) \Gamma_A^T = -x\left(t_{go}\lambda^T B_g \Phi + \mu^T\right)\Gamma_A^T,$$
$$\dot{\hat{B}}^T = -\left(\nabla_{\tilde{B}} H\right) \Gamma_B^T = -u\left(t_{go}\lambda^T B_g \Phi + \mu^T\right)\Gamma_B^T, \tag{21}$$

with $\Gamma_A, \Gamma_B \in \mathbb{R}^{6\times6}$ being positive definite matrices. Closed-form solutions can be found using the "sweep" method by assuming the adjoint vectors have the form

$$\lambda = P_D D + \Lambda\alpha, \ \mu = P_m \tilde{x} + C\beta, \tag{22}$$

where $\alpha(t) : [0, \infty) \to \mathbb{R}^6$, $\beta(t) : [0, \infty) \to \mathbb{R}^6$, and $\Lambda, C, P_m, P_D \in \mathbb{R}^{6\times6}$. Substituting them into (20) yields the following conditions

$$P_D A_g + A_g^T P_D + Q_D = 0, \ P_m A_m + A_m^T P_m + Q_m = 0,$$
$$\Lambda = -\nu_D A_g^{-T} P_D, \ C = -\nu_m A_m^{-T} P_m, \tag{23}$$
$$\alpha = t_{go} B_g \Phi\left(\hat{A}x + \hat{B}u\right), \ \beta = \hat{A}x + \hat{B}u,$$

where $\nu_D \geq 0$, $\nu_m \geq 0$ are free design parameters that enable balancing between robustness and performance of the parameter update laws. Finally, using (21), one can write them as

$$\dot{\hat{A}} = -\Gamma_A \left(t_{go}\Phi^T B_g^T P_D D + P_m \tilde{x} - \left(\nu_D t_{go}^2 \Phi^T B_g^T A_g^{-T} P_D B_g \Phi + \nu_m A_m^{-T} P_m\right)\left(\hat{A}x + \hat{B}u\right)\right)x^T,$$
$$\dot{\hat{B}} = -\Gamma_B \left(t_{go}\Phi^T B_g^T P_D D + P_m \tilde{x} - \left(\nu_D t_{go}^2 \Phi^T B_g^T A_g^{-T} P_D B_g \Phi + \nu_m A_m^{-T} P_m\right)\left(\hat{A}x + \hat{B}u\right)\right)u^T. \tag{24}$$

As can be seen, setting $\nu_D = \nu_m = 0$ in (24) would yield update laws (17).

4. Adaptive Coordination

4.1 Graph Theory Notions

The communication network of N receiver aircraft that exchange information with the tanker during an A3R operation can be described by an undirected connected graph defined as a triplet $\mathcal{G} = \{\mathcal{V}, \mathcal{E}, \mathcal{A}\}$, where $\mathcal{V} = \{n_1, n_2, \ldots, n_N\}$ is a node set, $\mathcal{E} = \{(n_i, n_j) \in \mathcal{V} \times \mathcal{V}\}$ is an edge set with the element (n_i, n_j) describing the communication from node n_i to node n_j, and $\mathcal{A} = [a_{ij}] \in \mathbb{N}^{N \times N}$ is the adjacency matrix. The edge $(j, i) \in \mathcal{E}$ states that receiver i has access to the information of receiver j, and is known as an incoming communication link to receiver i. Neighbours of receiver i are defined by the set $\mathcal{N}_i = j : (j, i) \in \mathcal{E}$ of all nodes with directed edges toward i. The adjacency matrix $\mathcal{A}$ is defined by $a_{ij} = 1$ if $(j, i) \in \mathcal{E}$, and $a_{ij} = 0$ otherwise. The Laplacian $L = [l_{ij}] \in \mathbb{N}^{N \times N}$ associated to the graph G is defined as $l_{ij} = \sum_{j=1, j\neq i}^{N} a_{ij}$ and $l_{ij} = -a_{ij}$, $i \neq j$. From this definition it is straightforward to conclude that $\lambda_L = 0$ is an eigenvalue of L and the vector of ones of size N, 1_N, is its associated eigenvector. When all of the receivers have access to the status of all of their neighbours within a graph, $\mathcal{E} = \mathcal{V} \times \mathcal{V}$ and the graph $\mathcal{G}$ is said to be complete.

4.2 Adaptive Second-order Consensus Protocol

For the special case of the A3R operation without communication link losses, $\mathcal{G}_{A3R}(t)$ is a cluster graph formed from the disjoint union of complete graphs $\mathcal{G}_{TP}(t)$, $\mathcal{G}_{EL}(t)$ and $\mathcal{G}_{ER}(t)$, which are associated to those formations of receiver aircraft located at the *Transition Position*, at *Echelon Left*, and at *Echelon Right* respectively, as shown in Figure 1. This cluster separation is intended to avoid cross couplings between receivers of different formations, to minimize the propagation of atmospheric disturbances along the network, and to restrict coordination to those agents who belong to the same formation.

Given a formation cluster f of $N_f(t) \in \mathbb{N}_{\geq 2}^{+}$ heterogeneous receiver aircraft defined by a switching complete graph $\mathcal{G}_f(t) = \{\mathcal{V}_f(t), \mathcal{E}_f(t), \mathcal{A}_f(t)\} \in \mathcal{G}_{A3R}(t)$ such that $i \in \mathcal{N}_f(t)$ with $\mathcal{N}_f(t)$ a subset containing all aircraft in the formation f, the second order autopilot dynamics of the i-th receiver aircraft defined by the pair A_i, B_i, with the nonlinear dynamic inversion guidance command (10) $u_i^G \in R^3$, and a consensus command denoted by $u_i^C \in R^3$ can be formulated as,

$$\begin{cases} \dot{x}_i = A_i x_i + B_i \left(u_i^G + u_i^C \right) \\ y_i = x_i \\ z_i = S_C x_i \end{cases} \quad \forall i \in \mathcal{N}_f(t) = \left\{ 1, \ldots, N_f(t) \right\}, \tag{25}$$

where $z_i \in \mathbb{R}^{n_c}$ is a consensus vector of variables representing $n_c \in \mathbb{N}_{>0}$ quantities of interest which are common to all receivers, and $S_C \in \mathbb{R}^{n_c \times 6}$ is a selection matrix. The consensus command u_i^C must be designed to make all z_i vectors of the receiver aircraft within a cluster graph G_i to converge to a common solution plus an agent-specific bias term. Moreover, to avoid a contest between guidance and coordination, the consensus command u_i^C must generate intra-formation flock behaviour patterns aligned with the guidance commands u_i^G.

In order to solve this problem, a second-order consensus protocol with the decoupling approach defined in [10], entailing additional stability modifications to the individual estimated parameters update laws (24) is proposed:

$$u_i^C = \left(\phi_i S_C \hat{B}_i \right)^{-1} \left(\phi_i \left(\dot{q}_i + A_c \left(S_C x_i - q_i \right) \right) - F_i \right) \quad \forall i \in \mathcal{N}_f(t) = \left\{ 1, \ldots, N_f(t) \right\}, \tag{26}$$

$$\dot{q}_i = K_L \sum_{j \in \mathcal{N}_{f_i}(t)} \left(\left(q_i - \delta_i \right) - \left(q_j - \delta_j \right) \right) + K_R \left(\left(q_i - \delta_i \right) - r_c \right) \quad \forall i \in \mathcal{N}_f(t) = \left\{ 1, \ldots, N_f(t) \right\}, \tag{27}$$

where $\mathcal{N}_{f_i}(t)$ is the subset of $\mathcal{N}_f(t)$ including all neighbours of agent i, $q_i \in \mathbb{R}^3$ is a vector containing the opinion of receiver aircraft i, $\delta_i \in \mathbb{R}^3$ is a bias vector to be determined, $r_c \in \mathbb{R}^3$ is the design reference vector, $A_C \in \mathbb{R}^{3 \times 3}$, $K_R \in \mathbb{R}^{3 \times 3}$ and $K_L \in \mathbb{R}^{3 \times 3}$ are diagonal negative definite design matrices, and $\phi_i = \Phi_i \left[0_{3 \times 3}^T \mid I_{3 \times 3}^T \right]^T$. It is worth noting that (26) is only defined when $S_C \hat{B}_i$ is regular, so n_c must be equal to the dimension of u, this is, the number of receiver aircraft autopilot commands, thus $n_c = 3$. Moreover, the nonsingular condition for $S_C \hat{B}_i$ restricts the selected coordination quantities present in z_i to those state variables in x_i that can be controlled directly through the control inputs. As $\hat{B}_i \triangleq [0_{3 \times 3} \mid \hat{B}_{R_i}^T]^T$, and assuming that $\hat{B}_{R_i}$ is regular, this condition can only be satisfied if we choose $S_C = [0_{3 \times 3} \mid I_{3 \times 3}]$ to obtain a consensus vector $z_i = S_C x_i = [\dot{v}_i, \dot{\chi}_i, \dot{\gamma}_i]^T$.

Redefining (27) for the whole formation f using $q \triangleq [q_1^T, q_2^T, \ldots, q_{N_f}^T]^T \in \mathbb{R}^{3N_f}$, $\Delta \triangleq [\delta_1^T, \delta_2^T, \ldots, \delta_{N_f}^T]^T \in \mathbb{R}^{3N_f}$, and $\vartheta = q - \Delta \in \mathbb{R}^{3N_f}$ as auxiliary variables yields

$$\begin{aligned}
\dot{\vartheta} &= L \otimes K_L \vartheta + \left((I_{N_f} \otimes K_R)\vartheta - 1_{N_f} \otimes K_R r_c \right) - \dot{\Delta} \\
&= \left(L \otimes K_L + I_{N_f} \otimes K_R \right)\vartheta - 1_{N_f} \otimes K_R r_c - \dot{\Delta},
\end{aligned} \tag{28}$$

where $\otimes$ denotes the Kronecker product. As $L \cdot 1_{N_f} = 0_{N_f}$, it can be shown that equation (28) has a stable stationary solution defined by $\vartheta = 1_{N_f} \otimes r_c + \Omega^{-1}\dot{\Delta}$, where $\Omega = (L \otimes K_L + I_{N_f} \otimes K_R)$, if $\lim_{t\to\infty} \ddot{\Delta} = 0_{3\times 1}$. For this reason, the design matrices K_R and K_L have to be selected in a way such that Ω is always regular. As demonstrated in [11], the stability of the stationary solution of (28) is determined by the stability of the following subsystems:

$$A_l = \lambda_l K_L + K_R \quad \forall l \in \{1, \ldots, N_f(t)\}, \tag{29}$$

where λ_l are the non-zero eigenvalues of the Laplacian L. Given that $\mathcal{G}_f(t)$ is a complete graph, then $\lambda_l = N_f(t) \; \forall l \in \{1, \ldots, N_f(t)\}$. Moreover, as K_R and K_L are diagonal negative definite matrices, it is then concluded that the stationary solution is globally asymptotically stable and the receiver aircraft within formation f always achieve coordination with $\lim_{t\to\infty} q = 1_{N_f} \otimes r_c + \Delta + \Omega^{-1}\dot{\Delta}$.

Substituting (26), (27) and (10) in (25), we obtain the following equation for the consensus vector z_i of a receiver aircraft with unknown matrices A_i and B_i:

$$\begin{aligned}
\dot{z}_i &= \dot{q}_i + A_C\,(z_i - q_i) - \tilde{A}_i x - \tilde{B}_i \left(u_i^G + u_i^C \right) \\
&= K_L \sum_{j \in \mathcal{N}_{f_i}(t)} \left((q_i - \delta_i) - (q_j - \delta_j) \right) + K_R \left((q_i - \delta_i) - r_c \right) \\
&\quad + A_C\,(z_i - q_i) - \tilde{A}_i x - \tilde{B}_i \left(u_i^G + u_i^C \right) \quad \forall i \in \mathcal{N}_f(t) = \left\{1, \ldots, N_f(t)\right\}.
\end{aligned} \tag{30}$$

The design objective of generating intra-formation flock behaviour patterns aligned with the guidance commands can only be met if the neighbour-independent term in (30) makes $\dot{z}_i$ follow the original guidance dynamics with model errors (10). This is,

$$F_i = K_R \left((q_i - \delta_i) - r_c \right) + A_C\,(z_i - q_i) \quad \forall i \in \mathcal{N}_f(t) = \left\{1, \ldots, N_f(t)\right\}. \tag{31}$$

Selecting $r_c = 0_{3\times 1}$, we can finally compute the bias vector δ_i as

$$\delta_i = -K_R^{-1}\left(F_i - A_C S_C x_i + (A_C - K_R)q_i \right) \quad \forall i \in \mathcal{N}_f(t) = \left\{1, \ldots, N_f(t)\right\}. \tag{32}$$

Once all terms in (26) and (27) have been defined, we know proceed to derive the new terms to be added to the estimated plant parameter update laws (24) and prove the stability of the guidance and consensus combination for the receiver aircraft in formation f using the following Lyapunov function:

$$V_C = \frac{1}{2} \sum_{i=1}^{N_f(t)} D_i^T P_D D_i + \frac{1}{2} \sum_{i=1}^{N_f(t)} \sigma_i^T P_C \sigma_i + \frac{1}{2} \sum_{i=1}^{N_f(t)} \tilde{x}_i^T P_m \tilde{x}_i + \frac{1}{2} \sum_{i=1}^{N_f(t)} \mathrm{tr}\!\left(\tilde{A}_i^T \Gamma_A^{-1} \tilde{A}_i\right) + \frac{1}{2} \sum_{i=1}^{N_f(t)} \mathrm{tr}\!\left(\tilde{B}_i^T \Gamma_B^{-1} \tilde{B}_i\right), \tag{33}$$

where $D_i = [d^T, \dot{d}^T]^T \in \mathbb{R}^6$ and $\sigma_i = S_C x_i - q_i$ are the guidance error vector and the consensus discrepancy of receiver aircraft i, respectively, and $P_C \in \mathbb{R}^{3\times 3}$, P_D, P_m, Γ_A, $\Gamma_B \in \mathbb{R}^{6\times 6}$ are positive definite matrices.

The guidance error dynamics (12) has to be modified for each receiver aircraft i to include the new consensus command (26). After some manipulations, the nonlinear guidance dynamic inversion error ε_{C_i} with consensus yields

$$\varepsilon_{C_i} \triangleq \ddot{d}_i + 2\xi_g \omega_g \dot{d}_i + \omega_g d_i = t_{go} \Phi_i \left(\tilde{A}_i x_i + \tilde{B}_i \left(u_i^G + u_i^C \right) \right) - K_L \sum_{j \in \mathcal{N}_{f_i}(t)} \left((q_i - \delta_i) - (q_j - \delta_j) \right),$$
$$\dot{D} = A_g D + B_g \varepsilon_{C_i}, \tag{34}$$

where A_g and B_g are defined in (12). The ordinary differential equation for the consensus discrepancy σ_i can be computed expressing equation (30) in terms of σ_i,

$$\dot{\sigma}_i = A_C \sigma_i - \tilde{A}_i x - \tilde{B}_i \left(u_i^G + u_i^C \right). \tag{35}$$

Using (9), (34) and (35), after collecting terms in $\tilde{A}_i$ and $\tilde{B}_i$, we obtain the time derivative of (33):

COOPERATIVE FORMATION FLYING CONTROL LAWS FOR AUTOMATIC AIR TO AIR REFUELLING

$$
\begin{aligned}
\dot{V}_C =& \frac{1}{2} \sum_{i=1}^{N_f(t)} D_i^T \left(P_D A_g + A_g^T P_D \right) D_i + \frac{1}{2} \sum_{i=1}^{N_f(t)} \sigma_i^T \left(P_C A_C + A_C^T P_C \right) \sigma_i + \frac{1}{2} \sum_{i=1}^{N_f(t)} \tilde{x}_i^T \left(P_m A_m + A_m^T P_m \right) \tilde{x}_i \\
&+ \sum_{i=1}^{N_f(t)} \mathrm{tr} \left(\tilde{A}_i^T \left(t_{go} \Phi_i^T B_g^T P_D D_i x_i^T + P_m \tilde{x}_i x_i^T - P_c \sigma_i x_i^T + \Gamma_A^{-1} \dot{\hat{A}}_i \right) \right) \\
&+ \sum_{i=1}^{N_f(t)} \mathrm{tr} \left(\tilde{B}_i^T \left(t_{go} \Phi_i^T B_g^T P_D D_i \left(u_i^G + u_i^C \right)^T + P_m \tilde{x}_i \left(u_i^G + u_i^C \right)^T - P_c \sigma_i \left(u_i^G + u_i^C \right)^T + \Gamma_B^{-1} \dot{\hat{B}}_i \right) \right) \\
&+ \sum_{i=1}^{N_f(t)} \mathrm{tr} \left(K_L^T B_g^T P_D D \sum_{j \in \mathcal{N}_{f_i}(t)} \left((q_i - \delta_i) - (q_j - \delta_j) \right)^T \right).
\end{aligned}
\tag{36}
$$

To grant that the first three terms in (36) related to the guidance, consensus and model errors remain negative, in addition to (15), another Lyapunov equation arises,

$$
P_C A_C + A_C^T P_C = -Q_C,
\tag{37}
$$

in which $Q_C \in \mathbb{R}^{3 \times 3}$ is a positive definite matrix. Moreover, using (36) we can obtain the new consensus-aware update laws for $\hat{A}_i$ and $\hat{B}_i$ as

$$
\begin{aligned}
\dot{\hat{A}}_i &= \Gamma_A \left(-t_{go} \Phi_i^T B_g^T P_D D_i x_i^T - P_m \tilde{x}_i x_i^T + P_c \sigma_i x_i^T \right) \\
\dot{\hat{B}}_i &= \Gamma_B \left(-t_{go} \Phi_i^T B_g^T P_D D_i \left(u_i^G + u_i^C \right)^T - P_m \tilde{x}_i \left(u_i^G + u_i^C \right)^T + P_c \sigma_i \left(u_i^G + u_i^C \right)^T \right).
\end{aligned}
\tag{38}
$$

Substituting (37) and (38) in (36) and reverting the trace operator yields

$$
\dot{V}_C = -\frac{1}{2} \sum_{i=1}^{N_f(t)} D_i^T Q_D D_i - \frac{1}{2} \sum_{i=1}^{N_f(t)} \sigma_i^T Q_C \sigma_i - \frac{1}{2} \sum_{i=1}^{N_f(t)} \tilde{x}_i^T Q_m \tilde{x}_i + \sum_{i=1}^{N_f(t)} \sum_{j \in \mathcal{N}_{f_i}(t)} \left((q_i - \delta_i) - (q_j - \delta_j) \right)^T K_L^T B_g^T P_D D_i.
\tag{39}
$$

In order to show that D_i, σ_i and $\tilde{x}_i$ are bounded, we need to further manipulate the last term in (39),

$$
\begin{aligned}
\varrho_i^T &= \sum_{j \in \mathcal{N}_{f_i}(t)} \left((q_i - \delta_i) - (q_j - \delta_j) \right)^T K_L^T, \\
\rho &\triangleq \left[\varrho_1, \varrho_2, \ldots, \varrho_{N_f} \right] = L \otimes K_L \vartheta.
\end{aligned}
\tag{40}
$$

The time derivative of ρ can then be calculated as,

$$
\dot{\rho} = L \otimes K_L \left(\rho + I_{N_{f_i}} \otimes K_R \vartheta - \dot{\Delta} \right),
\tag{41}
$$

and the stability of the system is defined by the stability of $\lambda_l K_L$. Once again, as $\mathcal{G}_f(t)$ is a complete graph, then $\lambda_l = N_f(t) \; \forall l \in \{1, \ldots, N_f\}$ and thus $L \otimes K_L$ is Hurwitz. Moreover, using (28), it follows that the system (41) has an asymptotically stable solution defined by $\lim_{t \to \infty} \rho = (L \otimes K_L) \Omega^{-1} \dot{\Delta}$ if $\lim_{t \to \infty} \ddot{\Delta} = 0_{3 \times 1}$. Then, there exist a t^* such that $\|\rho(t)\| \leq \|(L \otimes K_L) \Omega^{-1}\| \|\dot{\Delta}(t)\| + k$, for $t > t^*$ and $k > 0$ sufficiently small. Moreover, as $\|\dot{\delta}_i(t)\|$ is proportional to $\|\dot{x}_i\|$, and $\|\dot{\delta}_i(t)\| \leq \alpha \|\dot{x}_i\|$, with $\alpha \in \mathbb{R}^+$, we can state that $\|\varrho_i(t)\| \leq \lambda_{\max}((L \otimes K_L) \Omega^{-1}) \alpha \|\overline{p_i}\| + k$, where $\|\overline{p_i}\|$ is the upper bound of $\|\dot{x}_i\|$ and $\lambda_{\max}$ is the maximum eigenvalue. From these assumptions we obtain:

$$
\begin{aligned}
\dot{V}_C \leq& -\frac{1}{2} \sum_{i=1}^{N_f(t)} \lambda_{\min}(Q_D) \|D_i\| - \frac{1}{2} \sum_{i=1}^{N_f(t)} \lambda_{\min}(Q_C) \|\sigma_i\| - \frac{1}{2} \sum_{i=1}^{N_f(t)} \lambda_{\min}(Q_m) \|\tilde{x}_i\| \\
&+ \sum_{i=1}^{N_f(t)} \left(\lambda_{\max}((L \otimes K_L) \Omega^{-1}) \alpha \|\overline{p_i}\| + k \right) \lambda_{\max}(B_g^T P_D) D_i.
\end{aligned}
\tag{42}
$$

Given the following compact set,

$$\mathcal{S} = \Big\{ D_i \in \mathbb{R}^6, \sigma_i \in \mathbb{R}^3, \tilde{x}_i \in \mathbb{R}^6 : \frac{1}{2} \sum_{i=1}^{N_f(t)} \lambda_{\min}(Q_D) \|D_i\| + \frac{1}{2} \sum_{i=1}^{N_f(t)} \lambda_{\min}(Q_C) \|\sigma_i\| + \frac{1}{2} \sum_{i=1}^{N_f(t)} \lambda_{\min}(Q_m) \|\tilde{x}_i\|$$

$$- \sum_{i=1}^{N_f(t)} \Big(\lambda_{\max}((L \otimes K_L)\Omega^{-1})\alpha \|\overline{p_i}\| + k \Big) \lambda_{\max}(B_g^T P_D) D_i \leq 0, \tag{43}$$

$$\forall i \in \mathcal{N}_f(t) = \{1, \ldots, N_f(t)\} \Big\},$$

using (42) and (43), it can be shown that V_C decreases within the complementary set $\mathcal{S}_c$ and increases within the compact set $\mathcal{S}$ that contains $D_i = 0_{6 \times 1}$, $\sigma_i = 0_{3 \times 1}$ and $\tilde{x}_i = 0_{6 \times 1}$. Thus, any trajectory of these variables which starts within the compact set $\mathcal{S}$ will always stay inside it for all $t > t^*$. Therefore, applying LaSalle's Invariance Principle, we can conclude that D_i, σ_i and $\tilde{x}_i$ are ultimately uniformly bounded, and the proposed adaptive guidance and consensus laws are stable. It should be noted that with the proposed update laws in (38), it is not guaranteed that $\tilde{A}_i$ and $\tilde{B}_i$ will converge to $0_{6 \times 6}$ and $0_{6 \times 3}$ respectively, without an additional Presistence of Excitation condition.

5. Collision Avoidance Algorithm

The collision avoidance system propagates the trajectory of each aircraft within a time window $t \in [t_0, t_0 + t_H]$, where t_0 is the current instant, assuming that their geometric curvature and torsion remain constant. This operation yields an helix representing the approximate path that the vehicle will follow, with curvature k_h and torsion τ_h given by

$$k_h = \frac{\|v_0 \times a_0\|}{\|v_0\|^3} = \frac{\sqrt{\dot{\chi}_0^2 \cos^2 \gamma_0 + \dot{\gamma}_0^2}}{v_0},$$

$$\tau_h = \frac{v_0 \cdot (a_0 \times j_0)}{\|v_0 \times a_0\|^2} = -\frac{\dot{\chi}_0 \sin \gamma_0}{v_0} + \frac{1}{k_h^2 v_0^3}\Big(\ddot{\chi}_0 \dot{\gamma}_0 \cos \gamma_0 - \ddot{\gamma}_0 \dot{\chi}_0 \cos \gamma_0 - \dot{\gamma}_0^2 \dot{\chi}_0 \sin \gamma_0 \Big). \tag{44}$$

If these two properties were to be considered constant from t_0 to $t_0 + t_H$, the TNB frame of the propagation helix can be calculated from the Frenet-Serret formulas as functions of the traversed arclength s_h, yielding

$$T_h(s_h) = \frac{\tau_h^2 + k_h^2 \cos\Big(s_h \sqrt{k_h^2 + \tau_h^2}\Big)}{k_h^2 + \tau_h^2} T_h^0 + \frac{k_h \sin\Big(s_h \sqrt{k_h^2 + \tau_h^2}\Big)}{\sqrt{k_h^2 + \tau_h^2}} N_h^0 + \frac{k_h \tau_h \Big(1 - \cos\Big(s_h \sqrt{k_h^2 + \tau_h^2}\Big)\Big)}{k_h^2 + \tau_h^2} B_h^0,$$

$$N_h(s_h) = -\frac{k_h \sin\Big(s_h \sqrt{k_h^2 + \tau_h^2}\Big)}{\sqrt{k_h^2 + \tau_h^2}} T_h^0 + \cos\Big(s_h \sqrt{k_h^2 + \tau_h^2}\Big) N_h^0 + \frac{\tau_h \sin\Big(s_h \sqrt{k_h^2 + \tau_h^2}\Big)}{\sqrt{k_h^2 + \tau_h^2}} B_h^0, \tag{45}$$

$$B_h(s_h) = T_h(s_h) \times N_h(s_h),$$

$$T_h^0 = \frac{v_0}{\|v_0\|}, \quad N_h^0 = \frac{v_0 \times (a_0 \times v_0)}{\|v_0\| \|a_0 \times v_0\|}, \quad B_h^0 = T_h^0 \times N_h^0.$$

Other meaningful properties of the helix are its radius ρ_h and its axis, defined by a point p_h and a unit vector u_h:

$$\rho_h = \frac{k_h}{\tau_h^2 + k_h^2}, \quad p_h = r_0 + \rho_h N_h^0, \quad u_h = \frac{\tau_h T_h^0 + k_h B_h^0}{\|\tau_h T_h^0 + k_h B_h^0\|}. \tag{46}$$

The kinematic relationships that define the position, velocity, acceleration and jerk vectors of a particle along an helicoidal trajectory can be computed once a user-supplied arclength function $s_h = s_h(t)$ is defined (for instance, $s_h(t) = v_0 \cdot (t - t_0)$):

COOPERATIVE FORMATION FLYING CONTROL LAWS FOR AUTOMATIC AIR TO AIR REFUELLING

$$r_h(t) = \frac{1}{k_h^2 + \tau_h^2} \left[\left(\tau_h^2 s_h + k_h^2 \frac{\sin\left(s_h \sqrt{k_h^2 + \tau_h^2}\right)}{\sqrt{k_h^2 + \tau_h^2}} \right) T_h^0 + k_h \left(1 - \cos\left(s_h \sqrt{k_h^2 + \tau_h^2}\right) \right) N_h^0 + k_h \tau_h \left(s_h - \frac{\sin\left(s_h \sqrt{k_h^2 + \tau_h^2}\right)}{\sqrt{k_h^2 + \tau_h^2}} \right) B_h^0 \right],$$

$$v_h(t) = \frac{ds_h}{dt} T_h(s_h),$$

$$a_h(t) = \frac{d^2 s_h}{dt^2} T_h(s_h) + k_h \left(\frac{ds_h}{dt} \right)^2 N_h(s_h),$$

$$j_h(t) = \left(\frac{d^3 s_h}{dt^3} - k_h^2 \left(\frac{ds_h}{dt} \right)^3 \right) T_h(s_h) + 3 k_h \frac{d^2 s_h}{dt^2} \frac{ds_h}{dt} N_h(s_h) + k_h \tau_h \left(\frac{ds_h}{dt} \right)^3 B_h(s_h).$$

(47)

Once each propagation helix has been generated, the collision problem consists in finding the first zero of the following equation for each pair of aircraft $\{i, j\}$ in the formation,

$$\|r_{h,i}(t_{ij}) - r_{h,j}(t_{ij})\|^2 - \left(R_i + R_j \right)^2 \leq 0, \quad t_{ij} \in [t_0, t_0 + t_H],$$

(48)

where R_i is the radius that defines a safety sphere around the i-th vehicle. The solution to equation (48), which can be found using (47), $s_h(t)$ and any numerical root finding technique, will be the time-to-collide t_{ij} between the two considered aircraft. The absence of interference between the cylinders that contain each helix (augmented by the previously mentioned safety radiuses) can be tested for a fast return, namely,

$$d(p_{h,i} + \lambda u_{h,i}, \ p_{h,j} + \eta u_{h,j}) > \left(\rho_{h,i} + R_i \right) + \left(\rho_{h,j} + R_j \right) \implies \nexists \, t_{ij} \in [t_0, t_0 + t_H],$$

(49)

where $\lambda, \eta \in \mathbb{R}$ are the line parameters of each helix axis, and $d()$ is the Euclidean distance.

If found, the magnitude t_{ij} is then translated into a commanded velocity vector whose aim is to prevent a collision between the $\{i, j\}$ pair, with the form of what would be a symmetric repulsive force calculated at the collision instant t_{ij}, though applied at t_0 instead:

$$\Delta v_{cmd, i}^{CA\{i, j\}} = -\Delta v_{cmd, j}^{CA\{i, j\}} = f(t_{ij} - t_0) \frac{d_{ij} + b_{ij}}{\|d_{ij} + b_{ij}\|},$$

$$f(t_{ij} - t_0) = \frac{t_H}{\delta_1 (t_{ij} - t_0) + \delta_2} - \delta_3, \quad \delta_1 = \frac{1}{f_H + \delta_3} - \frac{\delta_2}{t_H}, \quad \delta_2 = \frac{t_H}{f_0 + \delta_3},$$

$$d_{ij} = \frac{r_{h,i}(t_{ij}) - r_{h,j}(t_{ij})}{\|r_{h,i}(t_{ij}) - r_{h,j}(t_{ij})\|},$$

$$n_{ij} = \left(e_{x/y/z} \times d_{ij} \right) / \|e_{x/y/z} \times d_{ij}\|,$$

$$b_{ij} = \left(\delta_4 + \frac{f(t_{ij} - t_0)}{\delta_5} \right) \frac{n_{ij} \times d_{ij}}{\|n_{ij} \times d_{ij}\|}.$$

(50)

In the expressions above, parameters δ_3, f_0 and f_H can be used to adjust the slope of the repulsive command and its values at $t_{ij} = t_0$ and $t_{ij} = t_0 + t_H$, respectively. Parameters δ_4 and $\delta_5 \gg 1$ control the bias vector b_{ij}, which must be used to deviate the commanded velocity increment from what a straight, pure repulsion would cause (one can choose between e_x, e_y, e_z or, in reality, any unit vector when calculating n_{ij} to tune the bias vector's direction); ϵ is some small numerical tolerance.

The complete collision avoidance velocity increment for the i-th aircraft will be the weighted average of all of the calculated pair-wise commands,

$$\Delta v_{cmd, i}^{CA} = \frac{\displaystyle\sum_{j \, : \, t_{ij} \in [t_0, t_0 + t_H]} \frac{1}{t_{ij} + \epsilon} \Delta v_{cmd, i}^{CA\{i, j\}}}{\displaystyle\sum_{j \, : \, t_{ij} \in [t_0, t_0 + t_H]} \frac{1}{t_{ij} + \epsilon}},$$

(51)

where ϵ is again a small constant. Finally, this velocity can be expressed in terms of a collision avoidance input u^{CA} through vector composition, taking into account the already known guidance and consensus inputs:

$$u^{CA} = \begin{bmatrix} v_T - u_1^{G+C} \\ \text{atan2}\left(\Delta v_{cmd}^{CA} \cdot e_y + u_1^{G+C} \sin u_2^{G+C} \cos u_3^{G+C}, \; \Delta v_{cmd}^{CA} \cdot e_x + u_1^{G+C} \cos u_2^{G+C} \cos u_3^{G+C}\right) - u_2^{G+C} \\ \text{asin}\left(\left(-\Delta v_{cmd}^{CA} \cdot e_z + u_1^{G+C} \sin u_3^{G+C}\right)/v_T\right) - u_3^{G+C} \end{bmatrix},$$

$$v_T = \sqrt{\left(\Delta v_{cmd}^{CA} \cdot e_x + u_1^{G+C} \cos u_2^{G+C} \cos u_3^{G+C}\right)^2 + \left(\Delta v_{cmd}^{CA} \cdot e_y + u_1^{G+C} \sin u_2^{G+C} \cos u_3^{G+C}\right)^2 + \left(\Delta v_{cmd}^{CA} \cdot e_z - u_1^{G+C} \sin u_3^{G+C}\right)^2},$$

$$u^{G+C} = u^G + u^C.$$

$$(52)$$

6. Simulation Results

The following autopilot model has been considered for a preliminary assessment of the proposed guidance scheme (10),

$$\dot{x} = \left[\begin{array}{c|c} 0_{3\times3} & I_{3\times3} \\ \hline -K & -C \end{array}\right] x + \left[\begin{array}{c} 0_{3\times3} \\ \hline K \end{array}\right] u, \tag{53}$$

where K, $C \in \mathbb{R}^{3\times3}$ are diagonal matrices, and the state and input vectors are the same as in (1). For this particular case, parameter update laws (24) can be simplified as

$$\dot{\hat{K}} = \Gamma_K \, \omega \left(x^T \left[\begin{array}{c} I_{3\times3} \\ \hline 0_{3\times3} \end{array}\right] - u^T\right),$$

$$\dot{\hat{C}} = \Gamma_C \, \omega \, x^T \left[\begin{array}{c} 0_{3\times3} \\ \hline I_{3\times3} \end{array}\right], \tag{54}$$

$$\omega = \left[\begin{array}{c|c} 0_{3\times3} & I_{3\times3} \end{array}\right]\left(t_{go}\Phi^T B_g^T P_D D + P_m \tilde{x} - \left(v_D t_{go}^2 \Phi^T B_g^T A_g^{-T} P_D B_g \Phi + v_m A_m^{-T} P_m\right)\left(\hat{A}x + \hat{B}u\right)\right).$$

Figures 2 and 3 show the time evolution of the miss distance vector, the estimated parameters, Lyapunov function (13) and commands u^G for a constant reference acceleration input a_{ref} combined with a constant lateral displacement r_{ref} (see equation (7)) contained in the North-East plane. It is apparent that $\dot{\hat{K}}$, $\dot{\hat{C}} \to 0$, but, without a sufficiently rich reference input, it cannot be guaranteed that $\hat{K} \to K$, $\hat{C} \to C$.
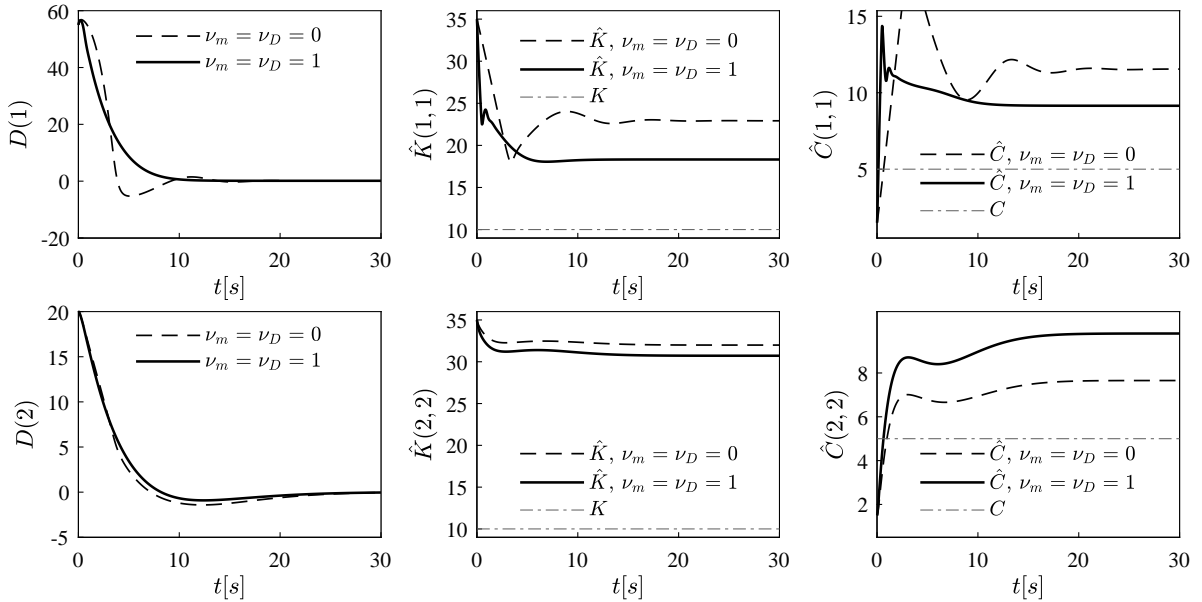

Figure 2: miss distance vector and estimated parameters.

Figure 4 depicts how the addition of consensus command (26) enables coordination of three heterogeneous plants, subjected to an additional disturbance representing atmospheric turbulence. In this case, all plant inputs are saturated reference velocity ramps.

COOPERATIVE FORMATION FLYING CONTROL LAWS FOR AUTOMATIC AIR TO AIR REFUELLING
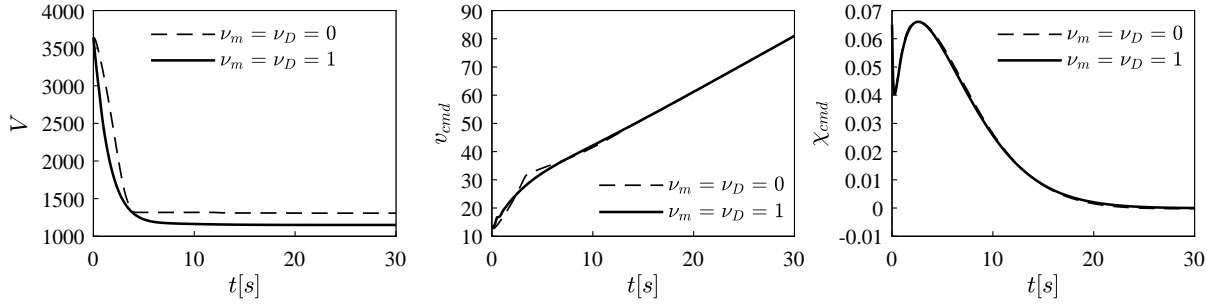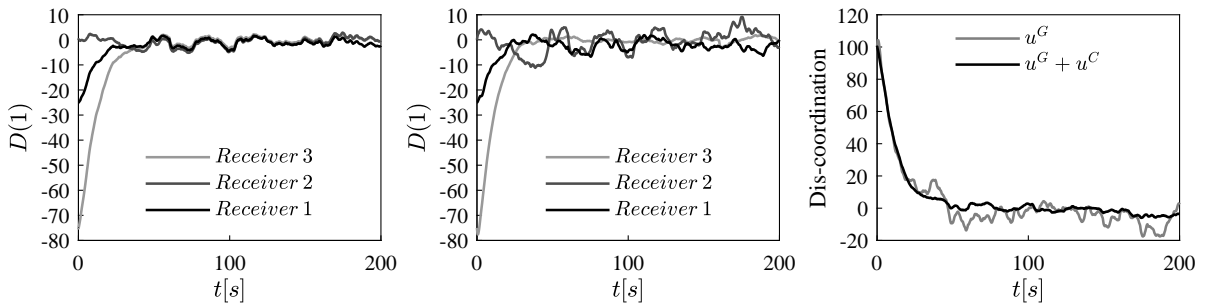

Figure 3: evolution of the Lyapunov function candidate and autopilot commands.

Figure 4: simulation results with turbulence comparing the receivers' miss distance when using $u^G + u^C$ (left) or just u^G (center). Dis-coordination measure when using $u^G + u^C$ or just u^G (right).

Finally, Figure 5 shows the trajectories of four plants when their autopilot commands include collision avoidance input (52), and are guided towards each other with constant and opposite v_{ref}. Results show that all collisions between them are effectively avoided, and the safety sphere around each other is never violated. In this case, the bias vector (see equation (50)) is calculated so that all trajectories remain in the North-East plane, for the sake of clarity.
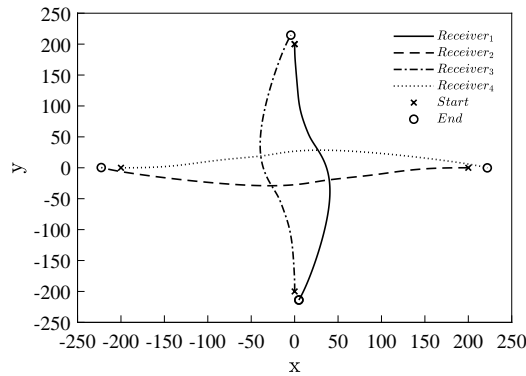
Figure 5: trajectories in a collision scenario (albeit operationally improbable in A3R), plant inputs are $u^G + u^{CA}$.

7. Conclusions and Future Work

This study describes the fully autonomous A3R Concept of Operation, analyzing it from a Flight Control Laws perspective. A tanker-centralized command and control architecture has been proposed, of which three key components have been identified and developed: an adaptive guidance law, a consensus protocol and a collision avoidance algorithm. Future work includes the development of a high-level manager in charge of overseeing and regulating each component output, and further research on alternative adaptive estimation techniques such as the promising Composite Learning Control [12, 13].

Abbreviations

A3R	Automatic Air to Air Refuelling
CCL	Cooperative Control Law
ARO	Air Refuelling Operator
AVO	Air Vehicle Operator
CONOPS	Concept of Operations
ARSAG	Aerial Refuelling Systems Advisory Group
LPV	Linear Parameter Varying

References

[1] Brian Dunbar. Nasa global hawks aid uav-to-uav refueling project, Jul 2015.

[2] Ryan Dibley, Michael Allen, and Nassib Nabaa. Autonomous airborne refueling demonstration phase i flight-test results. *AIAA Atmospheric Flight Mechanics Conference and Exhibit*, 2007.

[3] Airbus Defence and Space. Airbus achieves automatic air-to-air refuelling contact, May 2017.

[4] Airbus Defence and Space. Airbus performs world's first automatic air-to-air refuelling contact with large aircraft receiver, Jul 2018.

[5] Aerial Refuelling Systems Advisory Group. Automated aerial refueling concept of operations, Jun 2017.

[6] Brian D.O. Anderson. Adaptive systems, lack of persistency of excitation and bursting phenomena. *Automatica*, 21(3):247 – 258, 1985.

[7] Brian D.O. Anderson. Failures of adaptive control theory and their resolution. *Communications in Information and Systems*, 5(1):1–20, 2005.

[8] Byoung-Mun Min and Min-Jea Tahk. Three-dimensional guidance law for formation flight of uav. 2005.

[9] Nhan Nguyen and Sivasubramanya Balakrishnan. Bi-objective optimal control modification adaptive control for systems with input uncertainty. *IEEE/CAA Journal of Automatica Sinica*, 1:423–434, 10 2014.

[10] Gabriel Rodrigues de Campos, Lara Brinón-Arranz, Alexandre Seuret, and Silviu-Iulian Niculescu. On the consensus of heterogeneous multi-agent systems: a decoupling approach. *IFAC Proceedings Volumes*, 45(26):246 – 251, 2012. 3rd IFAC Workshop on Distributed Estimation and Control in Networked Systems.

[11] Simone Baldi, Ilario Azzollini, and Elias Kosmatopoulos. A distributed disagreement-based protocol for synchronization of uncertain heterogeneous agents. pages 2411–2416, 06 2018.

[12] N. Cho, H. Shin, Y. Kim, and A. Tsourdos. Composite model reference adaptive control with parameter convergence under finite excitation. *IEEE Transactions on Automatic Control*, 63(3):811–818, March 2018.

[13] Yongping Pan, Li Pan, and Haoyong Yu. Composite learning control with application to inverted pendulums. 11 2015.